AIAA 81-2035R

Prediction of Jet Exhaust Noise on Airframe Surfaces During Low-Speed Flight

L. M. Butzel*
Boeing Commercial Aircraft Company, Seattle, Washington

The behavior of pressure fluctuations measured on the airframe of a prototype high-lift jet transport (YC-14) is presented. Efforts to characterize the data in terms of a modest number of parameters and the resulting prediction procedures are described. Comparisons with near field engine exhaust noise of a conventional jet transport (Boeing 747) are presented. The results suggest that at low speeds the same exhaust noise source is important for both aircraft types. The results also suggest a consistent frequency sensitivity, as well as level sensitivity to airplane velocity. The frequency result appears to be new data.

Nomenclature

AFWAL	= Air Force Wright Aeronautical Laboratories
ALT	= airplane altitude
H	= nozzle hydraulic diameter
F	= frequency
L_{core}	= potential core length
N_1	= engine fan speed
QSRA	= quiet shorthaul research aircraft
s	= downstream distance of field point
SFP	= surface fluctuating pressure
STOL	= short takeoff and landing
TBL	= turbulent boundary layer
USB	= upper surface blowing
VGs	= vortex generators
$V_A, V_{A/P}$	= airplane velocity
V_{mix}	= jet exhaust mixed velocity
V_0	= reference velocity = 250 m/s
δ	= distance between field point and point of closest approach of flow stream to field point
ρ_{mix}	= jet exhaust mixed density
ρ_0	= reference density (sea-level ambient air)
θ_F, USB $\measuredangle$	= USB flap angle
θ_{FT}	= thrust flow turning angle
θ'	= flow idealization ribbon angle

Introduction

THIS paper describes highlights of five years of Boeing work aimed at characterizing pressure fluctuations acting on the airframe of jet powered transports. Such information is used to estimate sonic stresses and cabin noise levels. For these purposes, pressure fluctuations are considered to arise from turbulent boundary-layer (TBL) activity and engine noise. The present paper is limited to low-speed engine noise activity, arising from the interaction of the exhaust flow stream with the ambient air and/or directly with portions of the airframe. In addition, a companion paper presents material which deals with high-speed, high-altitude engine noise.[1]

A major part of the work discussed in this paper centers around the YC-14 transport aircraft. This airplane, which was built by Boeing for the U.S. Air Force as a part of its advanced medium short takeoff and landing (STOL) transport development program, flew for the first time in mid-1976 (Fig. 1). It was the first to employ upper surface blowing (USB) to achieve its STOL capability. In the period from 1975 to 1979, an extensive full-scale ground rig and airplane ground and flight data base was acquired and verified, with added funds provided by U.S. Air Force (AFWAL) and NASA, and by Boeing.[2-4] Thereafter, the data base was quite successfully correlated against a modest number of airplane configuration and operating parameters, and a prediction procedure for USB-STOL transports was developed.[5,6]

The most important low-speed engine source component emerging out of this effort was "jet mixing noise." An important feature of this source is its frequency sensitivity to both engine exhaust velocity and airplane forward speed. The frequency sensitivity to airplane forward velocity is a feature that we have not been aware of before.

Comparisons with data for a conventionally configured jet transport, a Boeing 747, have also been carried out as part of the data analysis effort.[5] Originally this effort was aimed at clarifying differences amongst these configuration types. However, it is now felt that of even more importance has been the identification of similarities, and hence the applicability of aspects of the YC-14 prediction technology to conventional transports. Based on this comparison, the component developed from the YC-14 data base appearing to carry over to conventionally configured jet transports during low-speed operations is jet mixing noise.

YC-14 Test Program

A description of the test program during which surface fluctuating pressure (SFP) was measured was presented in 1977 at the AIAA/NASA V/STOL Conference[7] and at the AIAA 4th Aeroacoustics Conference.[8] Briefly, measurements were made on the No. 1 airplane. This airplane used two 51,000-lb-thrust rated CF6-50 engines (bypass ratio ~ 5) mounted close to the fuselage in an overwing configuration. With this arrangement the engine exhaust flow remained attached to the USB flaps even when they were rotated downward (Coanda effect). With the help of flow spreading doors built into the outboard side of each nozzle, and vortex generators (Fig. 2), flow attachment could be maintained to large USB flap angles. This resulted in large flow turning and a high-capability, highly controllable powered lift system.

Measurements were also made on a ground test rig (Fig. 3) that used an engine, nacelle, and flaps destined for the No. 2 airplane, all coupled to a simulated section of fuselage.

SFP instrumentation consisted of flush microphones on fuselage, wing, and flap surfaces (Figs. 4 and 5). A somewhat greater number of microphones was installed on the ground test rig.

In addition to this instrumentation, static pressure probes, thermocouples, accelerometers, and interior microphones were also used to assess other aspects of the YC-14's USB-STOL environment.[5]

Presented as Paper 81-2035 at the AIAA 7th Aeroacoustics Conference, Palo Alto, Calif., Oct. 5-7, 1981; submitted Oct. 14, 1981; revision received March 11, 1982.

*Lead Engineer, Cabin Noise Research.

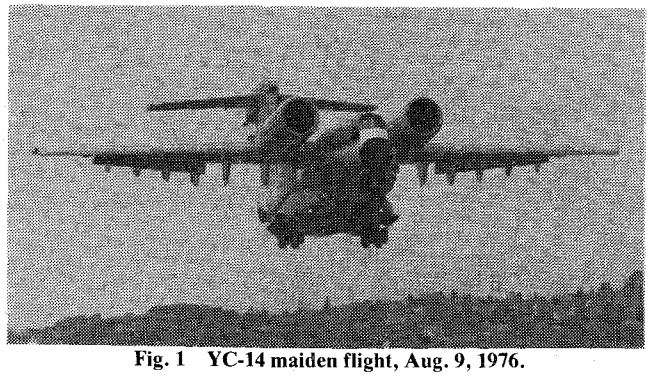

Fig. 1 YC-14 maiden flight, Aug. 9, 1976.

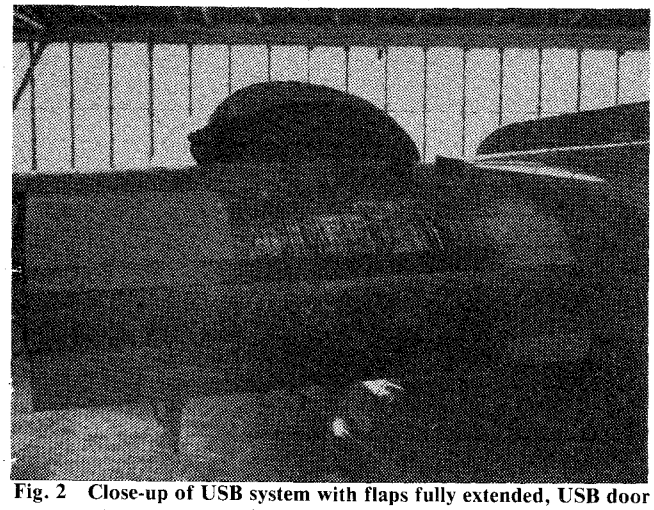

Fig. 2 Close-up of USB system with flaps fully extended, USB door open, vortex generators raised.

Ground rig data were obtained at various power settings, flap positions, vortex generator positions, and nozzle door position combinations. All these functions were independently controllable on the ground rig.

Flight test conditions were chosen to cover the operating envelope of the airplane, as indicated schematically in Fig. 6. A number of simulated STOL approaches, the 30,000-ft (10-km) conditions and the USB flap cycle condition were flown specifically to support the assessment of SFP. The USB flap cycle condition involved a slow lowering, then raising of the USB flaps (about 1 min duration), during which airplane speed and power setting were held fixed. Various ground conditions (with the airplane stationary) involving one or both engines operating were also run, complementing many runs accomplished on the ground test rig.

Test Results and Trends

The number of one-third-octave-band SFP spectra produced during the YC-14 test program exceeded 4000. About half this number of narrow-band spectra were also generated. On the whole, these were quite free of strong narrow-band spikes. Hence attention was focused exclusively on understanding the more compact one-third-octave-band spectra. Figures 7-11 illustrate the main characteristics of SFP on the YC-14 associated with its propulsion system.

Figure 7, in conjunction with Fig. 5, illustrates the following static or low-speed, low-altitude features.

1) The spectral levels exhibit a simple, single-peaked, gently rolling-off shape at all fuselage points close to or scrubbed by the jet mixing region of the exhaust flowfield.

2) Points near to and below the trailing edge of the USB flaps often exhibit a low-frequency deviation from the item 1 characterization.

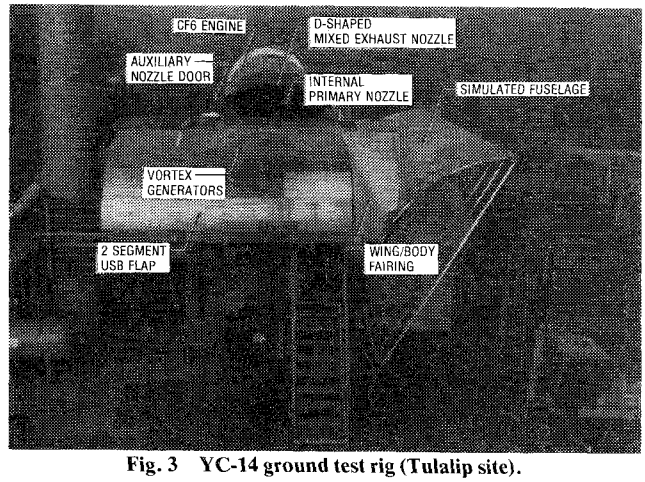

Fig. 3 YC-14 ground test rig (Tulalip site).

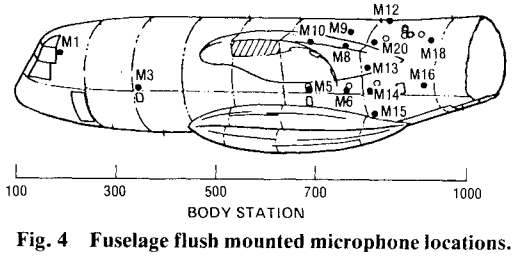

Fig. 4 Fuselage flush mounted microphone locations.

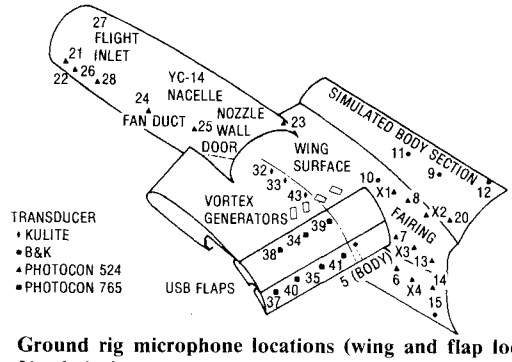

Fig. 5 Ground rig microphone locations (wing and flap locations same on No. 1 airplane).

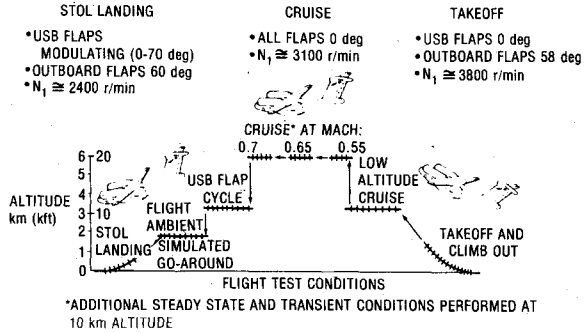

Fig. 6 Flight test measurement conditions.

3) There is a strong inverse dependence of (peak) levels on distance from the intuitively expected location of the flowfield.

Figure 8 also illustrates spectral changes associated with changes in position of the flowfield (which is dependent upon position of the USB flaps). It also illustrates the distinct changes observed when vortex generators (VGs) are deployed. The behavior at point M15 (Fig. 4) is suggestive of the approach of a noise source—such as the exhaust flowfield

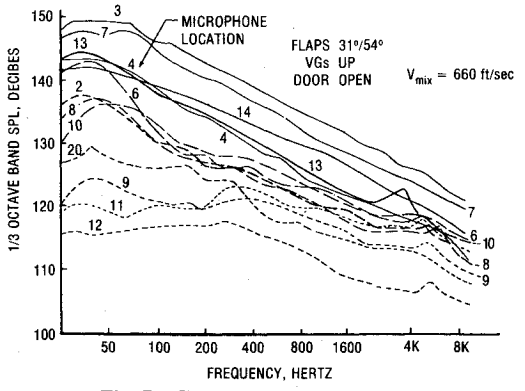

Fig. 7 Ground rig fuselage spectra.

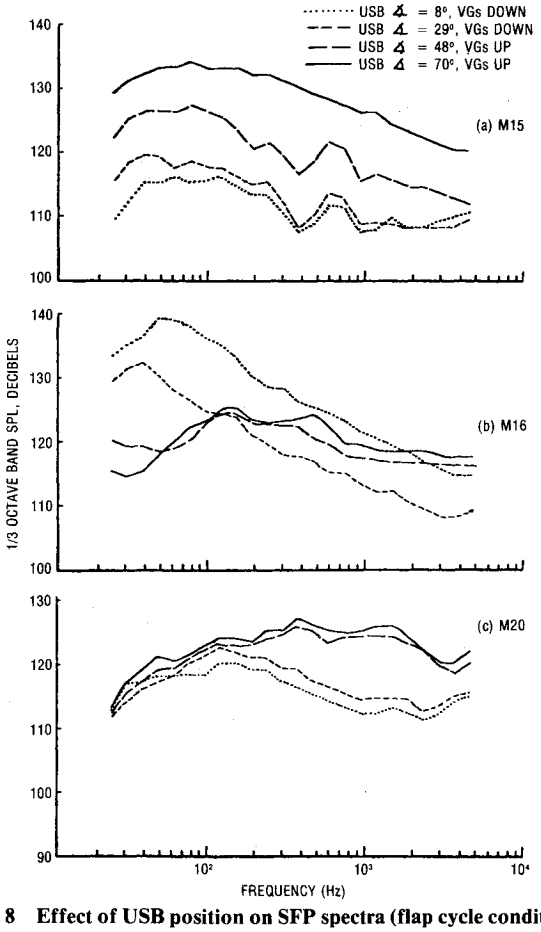

Fig. 8 Effect of USB position on SFP spectra (flap cycle condition).

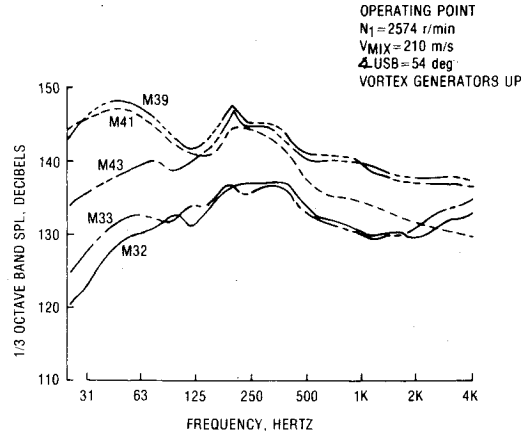

Fig. 9 Wing and flap SFP spectra.

mixing region. At M16, it is suggestive of the departure of the same source, except for a distinct modification association with VG deployment. The behavior at M20, which is yet further removed from the turning portion of the flow stream, exhibits less sensitivity, but still shows the distinct effect of the VGs.

For the wing and flap region scrubbed by the exhaust flow, Fig. 9 is interpreted as showing behavior consistent with that on the fuselage. However, owing to their location, VG effects are even stronger here than on the fuselage.

The effect of low-speed airplane forward velocity is illustrated in Fig. 10. This behavior, observed during a takeoff where the engine power was held constant, indicates that 1) peak levels decrease with increasing forward velocity, or with decreasing relative jet velocity; 2) the frequency of the peak level increases with increasing airplane velocity.

Figure 11 compares the effect of engine power setting (exhaust jet velocity) on spectral levels at low-speed, low-altitude operation. In this case, airplane speed was held constant. These spectra also suggest a dependence of the frequency of peak level on airplane velocity.

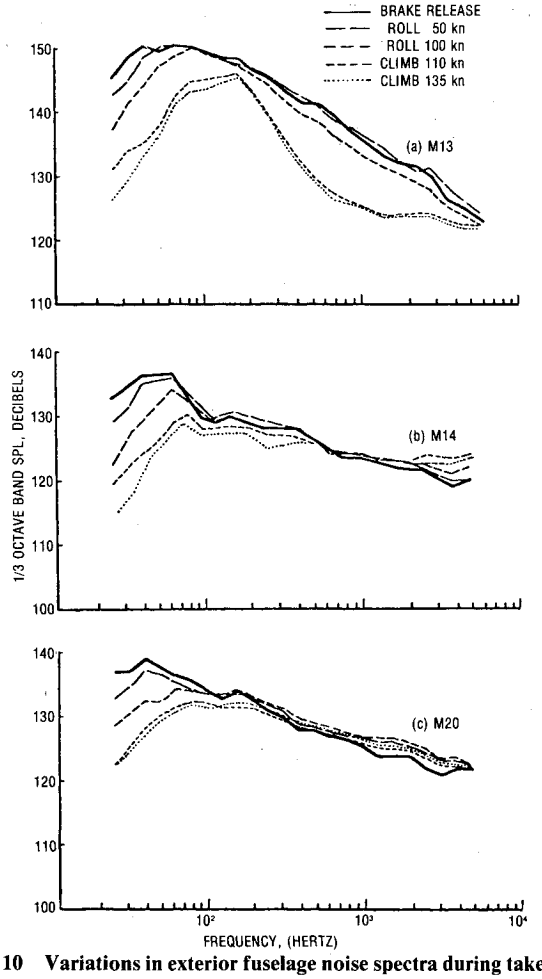

Fig. 10 Variations in exterior fuselage noise spectra during takeoff.

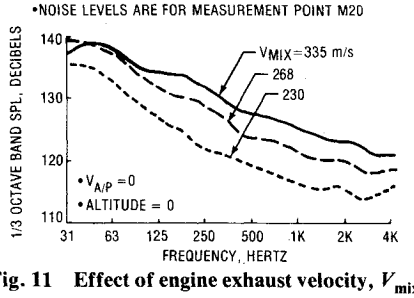

Fig. 11 Effect of engine exhaust velocity, V_{mix}.

Data Correlation—General View

The behavior illustrated in Figs. 7-11 was interpreted in the following manner.

1) Low-speed, low-altitude SFP is primarily controlled by a jet exhaust mixing noise source for which the following parameters are important: the distance from the mixing stream region approaching closest to the field point (δ); the relative jet velocity ($V_{mix} - V_A$); the airplane velocity and jet velocity (V_A, V_{mix}); the distance of the field point downstream of the engine nozzle exit plane (s); and the exhaust stream fluid density (ρ_{mix}).

2) The effect of deployed VGs is to amplify a (frequency) portion of the jet mixing noise source spectrum. The effect is strongest for points on wing and flap where the VGs are located.

3) Other sources need to be considered, particularly for field points close to flap trailing-edge areas, for example, those due to flow interaction with flap edges or flow separation associated with large USB flap angles.

In the following discussion, only data correlations with regard to the views of item 1 are considered. Detailed discussion of these and the others are presented elsewhere.[1,5,6]

Flowfield Idealization

Figure 12 shows the exhaust flowfield and geometry idealization adopted for the YC-14's propulsion setup. In this idealization the flow is viewed as a ribbon emanating from the nozzle and attached to the wing surface. It remains attached until separating from the USB flap at an angle θ' and continues on a straight course as that same angle. Based on other data, the inboard side of the flow ribbon is taken to be in contact with the fuselage at its widest point.

Evaluation of the flow idealization ribbon angle, θ', was accomplished using ground rig data taken at various USB flap settings and power settings. The approach (Fig. 13) consisted of locating by inspection a ribbon angle, θ', such that overall sound pressure levels (OASPLs) varied inversely with distance, δ, from the selected field points. Concurrent ground rig data on thrust flow turning, θ_{FT}, and USB flap angle, θ_F, and from scale model tests,[9] were then used to derive the relations shown in Fig. 14, relating θ_{FT} to θ_F, and thence θ' to θ_{FT}. In general, no particular dependence on power setting was anticipated or observed.

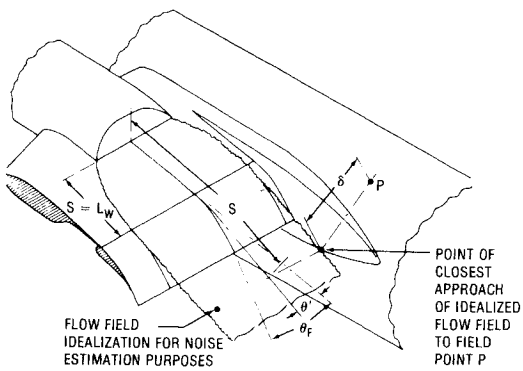

Fig. 12 YC-14 exhaust flow idealization.

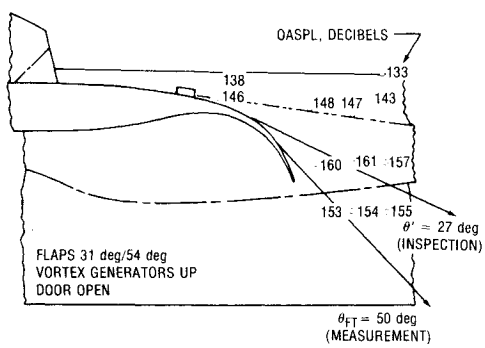

Fig. 13 Method of determining θ'.

Low-Speed, Low-Altitude Correlations

Figure 15 shows the success of the above approach in collapsing fuselage OASPLs. The field points considered in the figure all had normalized downstream distance coordinates, s/D_H, between 3 and 4. Subject to modest variations associated with USB flap angle effects, this figure also provided a basis for characterizing the dependence of spectral (peak) level on normalized distance away from the flow stream, δ/D_H. The frequency of the peak level was also found to increase with increasing δ/D_H.[5]

Figure 16 shows the characterization developed for peak level dependence on s/D_H corresponding to $\delta/D_H = 0$. Data for this used wing and flap field point spectral levels (like those in Fig. 9) as well as fuselage spectral levels (like those in Fig. 7).

The following relation for the effect of fluid density (mixed), jet velocity, and airplane velocity on peak spectral level was used.

$$\mathrm{SPL}_{peak}(\rho_{mix}, V_{mix}, V_A) = \mathrm{SPL}_{peak}(\rho_0, V_0, 0) + 10\log\left(\frac{\rho_{mix}}{\rho_0}\right)^2 + 10\log\left(\frac{V_{mix} - V_A}{V_0}\right)^4 \quad (1)$$

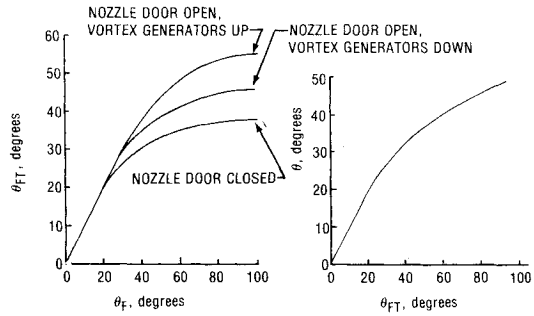

Fig. 14 Empirically derived relation between θ_F, θ_{FT}, and θ'.

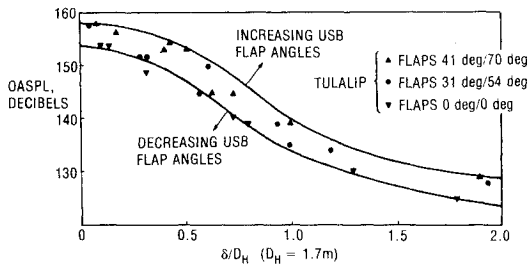

Fig. 15 Correlation between fuselage OASPLs and distance δ of field point from ribbon idealization.

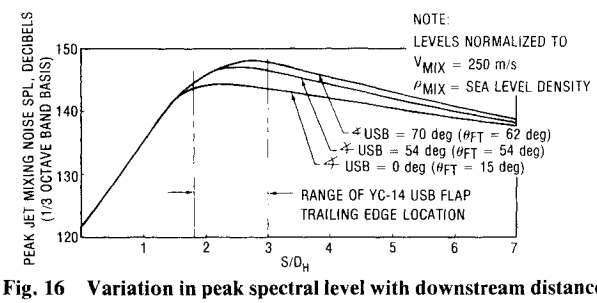

Fig. 16 Variation in peak spectral level with downstream distance.

This form was suggested[10] for use in the near field of jet exhaust mixing. The success of this relation is indicated in Fig. 17. It suggests that a higher velocity exponent (from 5 to 6) might have been in order for some fuselage field points. However, this is a change we have not introduced as yet.

For the frequency of the peak level under static conditions, and for field points scrubbed by the exhaust flow ($\delta/D_H = 0$), a form suggested by Filler[11] was used:

$$f^0_{\text{peak}} = \left(\frac{V_{\text{mix}}}{D_H}\right)\left(\frac{1.8}{s/D_H + 3}\right) \tag{2}$$

The success of this equation is shown in Fig. 18.

To account for effects of forward velocity on frequency of peak level, a form found to fit the data (Fig. 10) was

$$f_{\text{peak}}(V_A \neq 0) = f^0_{\text{peak}}\left(\frac{V_{\text{mix}} + V_A}{V_{\text{mix}}}\right)\left(\frac{V_{\text{mix}} + V_A}{V_{\text{mix}} - V_A}\right) \tag{3}$$

This expression is based on the view that the frequency of the most intense SFP at a field point close to the jet exhaust stream should be directly proportional to the speed eddies convected past the field point and inversely proportional to the size of these eddies. The eddy convection speed is taken to be of the order

$$\tfrac{1}{2}(V_{\text{mix}} + V_A)$$

The size of the eddies is taken to be relatable to s/L_{core}. In Eq. (3), L_{core} is taken to scale with

$$(V_{\text{mix}} + V_A)/(V_{\text{mix}} - V_A)$$

Finally, application of the various rules listed above, primarily to ground rig and airplane ground data for fuselage field points, yielded a characteristic spectrum shape for the dominant low-speed, low-altitude induced SFP (Fig. 19).

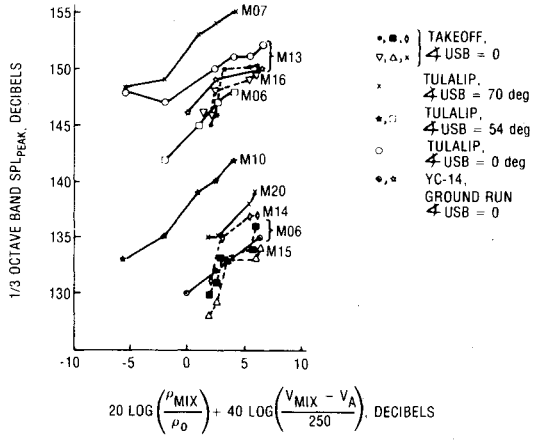

Fig. 17 Correlation of peak spectral level with Eq. (1).

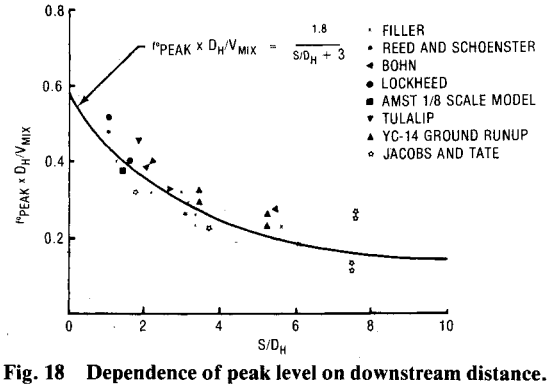

Fig. 18 Dependence of peak level on downstream distance.

USB-STOL Prediction Procedures

The flowfield characterization, dimensionless spectral shapes and scaling rules for peak levels, and frequency of peak levels define an interpolating procedure for SFP at any point on the YC-14.

To the degree that this model is strongly tied to measured YC-14 data, its ability to predict levels on (other) USB-STOL configured aircraft remains to be determined. In fact, at least two other USB-STOL airplanes are flying. One is the Quiet Shorthaul Research Aircraft (QSRA), built by Boeing under contract to NASA, and for which some SFP data are available. However, no checks against these data have yet been made. The other airplane is the Russian-built AN-72, for which we are not aware of any SFP data.

With these limitations in mind, the above interpolating procedures have been packaged into a formalized prediction procedure for USB-STOL configured transports.[5,6] As presented in these references, the procedure contains a number of sources beyond those discussed in this paper. All of these are indicated in Fig. 20. As in the case of jet mixing noise, each other source contains scaling rules for peak level and frequency of peak level and a dimensionless spectrum shape. In most cases the dimensionless spectra are empirical, while scaling rules are a blend of intuition, theory (literature), and empiricism. These other sources were all developed to account for spectral "residues" left after accounting for jet mixing noise.

A computerized version of this prediction package (interpolation package) has been developed. This included a plotting package coupled directly to a completely digitized one-third-octave band YC-14 SFP data base. Comparisons of predictions and data have been easy to make allowing for "trial-and-error trimming" of the prediction package. Typical examples of the degree of matching that has been achieved are shown in Figs. 21 and 22. These also illustrate the

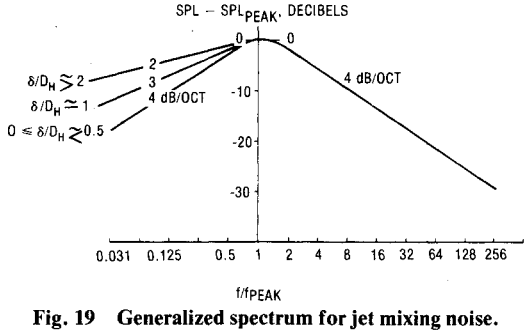

Fig. 19 Generalized spectrum for jet mixing noise.

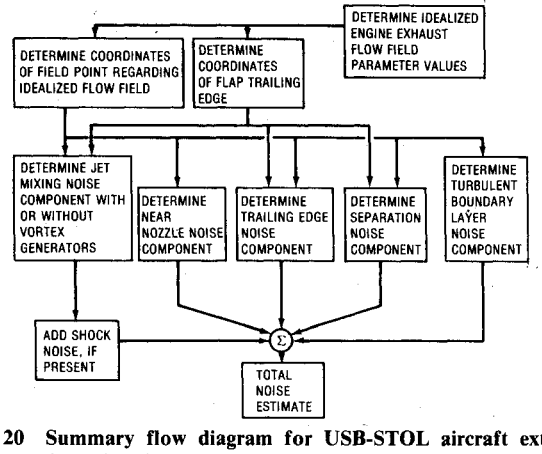

Fig. 20 Summary flow diagram for USB-STOL aircraft exterior surface noise estimation procedure.

typical degree to which jet mixing noise dominates the low-speed behavior.

Comparison with 747 Data

As part of the NASA and AFWAL funded analysis effort to characterize YC-14 SFP, comparisons with the behavior for a conventionally configured jet transport were briefly undertaken.[5] The most appropriate data available at Boeing for this purpose were those measured on a CF6-50 equipped Boeing 747 (Table 1). In particular, data were obtained for a series of field points on the lower wing surface outboard of an outboard engine (Fig. 23). Data were taken at each of about five power settings, with the airplane on the ground, and during several low-speed, low-altitude conditions and several high-speed, high-altitude conditions.

Figure 24 shows a sampling of ground operation spectra for comparable field points. Based upon δ/D_H and s/D_H scaling rules for the YC-14, a variation of from 3 to 5 dB in peak spectral levels would have been expected for the indicated range of δ/D_H. The figure has been interpreted as indicating that, below about 500 Hz, jet mixing noise for conventionally configured airplanes is similar to that for USB-STOL airplanes. Above 500 Hz, turbomachinery (TM) noise appears to be greater for the 747, perhaps owing to the much shorter length of its engines' fan ducts.

A more impressive suggestion of jet mixing noise similarity is provided by Fig. 25, in which the effect of forward velocity on low-speed, low-altitude 747 exhaust noise is shown. Shifts A and B are the frequency and amplitude shifts predicted by the USB-STOL relationships of Eqs. (1) and (3). In each of the two cases shown, the flight idle spectra (curve 3) is known to be TBL noise dominated.

At field point F07 (Fig. 23), the USB-STOL relationship performs well in the range anticipated to be jet mixing noise dominated, but not at higher frequencies where TM noise dominates. For field point F01, the shifted location of curve 1 falls below the idle curve 3, suggesting that for the power setting/airplane velocity combination considered, TBL noise

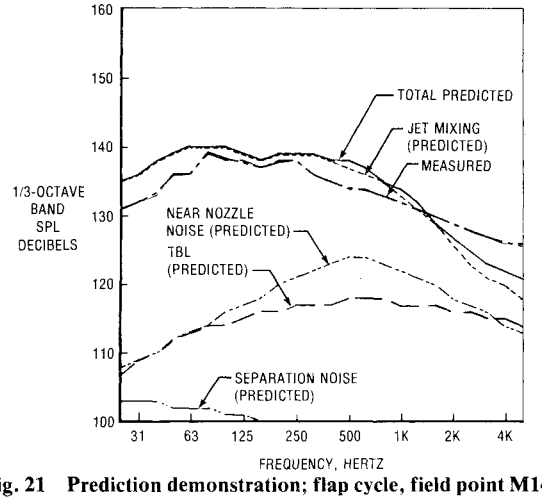

Fig. 21 Prediction demonstration; flap cycle, field point M14.

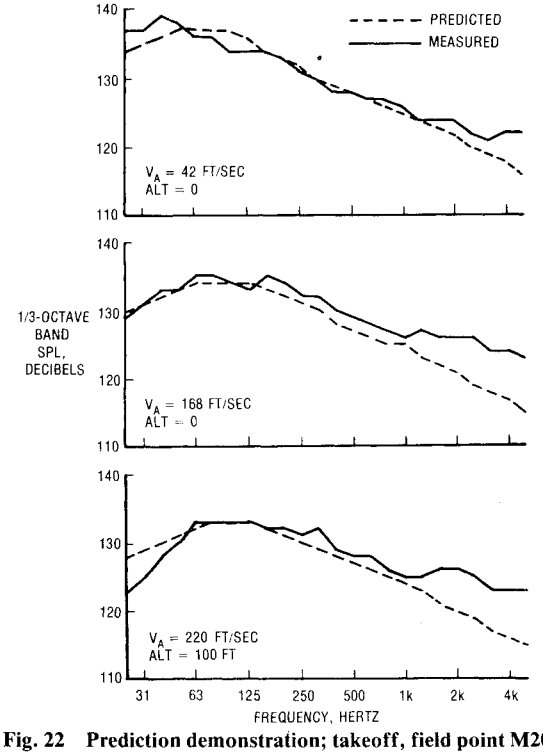

Fig. 22 Prediction demonstration; takeoff, field point M20.

Table 1 Important features of YC-14 and 747 regarding comparison of noise behavior

Item	YC-14	747
Propulsion configuration	USB/D-nozzle, CF6-50	Conventional pylon-mounted/circular nozzle, CF6-50
Primary	Retracted	Extended
Fan	Full-length duct	Short duct
Exterior microphones	Side and high fuselage sidewall	Lower wing surface (and window blanks)
Hydraulic diameter	1.7 m	1.7 m

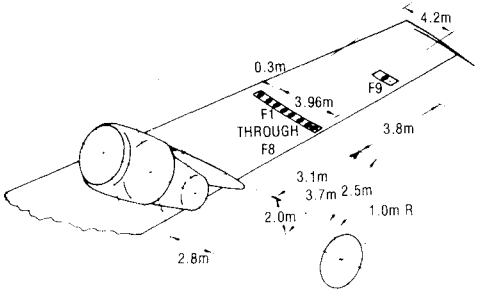

Fig. 23 747/CF6-50D core noise flight test underwing microphone locations (F1 through F9).

	SOURCE	S/D_H	δ/D_H	ALTITUDE (km)	V_A(m/s)	N_1 (r/min)	V_{MIX}(m/s)
——	747 (F07)	3.6	1.5	0	0	3360	296 (EST)
—□—	747 (F02)	1.7	1.5	0	0	3360	296 (EST)
- - - -	YC-14 (M12)	3.6	1.8	0	0	3150	271
—·—	YC-14 (M15)	3.6	1.3	0	0	3150	271
·····	YC-14 (M09)	2.8	1.1	0	0	3150	271

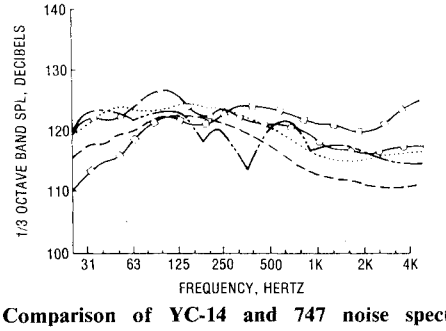

Fig. 24 Comparison of YC-14 and 747 noise spectra-ground operations.

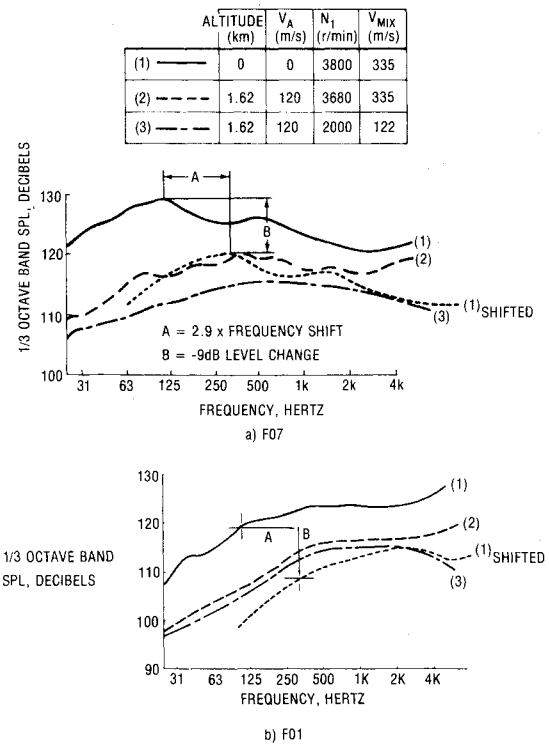

Fig. 25 Effectiveness of YC-14 forward velocity scaling relations when applied to 747 wing pod noise spectra.

is dominant at a field point location with $s/D_H \simeq 0$, $\delta/D_H \simeq 1.5$. Such behavior is consistent with observed YC-14 trends.

In retrospect, the observed similarities make good intuitive sense; jet mixing activity for two jet propulsion systems built around the same CF6-50 core/fan unit could well be expected to show the same first-order behavior. Taking obvious vortex generator and flow turning effects out of the picture, the remaining major effect influencing the behavior of these sources for the two configurations considered would be flow attachment to the wing and body (for the YC-14). The limited results shown suggest that to first-order flow, attachment is not a dominant factor either.

Concluding Remarks

The work described in this paper is felt to represent a first-order manipulation (analysis) of a quite large, highly consistent data base for the YC-14, USB-STOL transport. The analysis has invoked a blend of intuition, theory (literature), and empiricism. It has yielded a reasonably compact low-speed characterization of SFP on the YC-14 airframe in terms of 1) a particular jet exhaust flowfield idealization, and 2) one dominating source: jet mixing noise.

For this source, a generalized spectrum shape and scaling relations for the peak level and frequency of peak level have been developed. The frequency is found to depend upon jet exhaust velocity and on airplane velocity. The latter dependence appears to be new.

This source characterization, along with several others not discussed in this paper, has been formalized into a USB-STOL airplane SFP prediction package. The package shows consistent behavior with the YC-14 data base used to construct it. However, no checks against data for any other STOL airplane have yet been made.

A brief assessment of SFP data measured on a conventionally configured jet transport (Boeing 747) has also been described. The results of the effort have suggested that the jet mixing noise source characterization for the YC-14 has useful applicability to conventionally configured jet transports, like the 747.

Much of the work that has been described was accomplished on a best-effort contract basis. As such, the results are still considered to be more preliminary than we would like. This is particularly so with regard to conventionally configured transports. Additionally, more detailed evaluation of scaling rules against source YC-14 and 747 data bases, and against the literature is needed and is being planned.

As part of this effort, comparisons against other scaling rule/prediction formats are already in progress. For example, comparisons are being attempted with regard to the near field noise prediction package recently put together by Lockheed for NASA.[12-14] This package is based on a careful evaluation and selection of data and methods available in the literature as of mid-1978. The results of these further efforts will be the subject of a future report.

Acknowledgments

Funding for this work has been provided by the U.S. Air Force under Contract F33657-72-C-089 change P00023, P00026 and P00028, and under Contract F33615-77C-3035; the National Aeronautics and Space Administration under Contract NAS2-9328; and the Boeing Commercial Airplane Company, Seattle, Wash.

References

[1] Butzel, L.M., "Prediction of Jet Exhaust Noise on Airframe Surfaces During Flight," AIAA Paper 81-2035, Oct. 1981.

[2] Harkonen, D.L., Reed, J.B., and Sussman, M.B., "YC-14 Ground and Flight Experiments for NASA—Ground Test Final Report," Boeing Commercial Airplane Company Document D74810113-1, April 1976.

[3] Eldridge, W.M., Reed, J.B., and Sussman, M.B., "YC-14 Ground and Flight Experiments for NASA—Flight Test Final Report," Boeing Commercial Airplane Company Document D74810113-2, July 1977.

[4] Butzel, L.M., "YC-14 Interior Noise Measurements Program," AFFDL-TR-77-128, Dec. 1981.

[5] Butzel, L.M., Bohn, A.J., Armstrong, R.J., and Reed, J.B., "Noise Environment of Wing, Fuselage and Cabin Interior of a USB-STOL Airplane," NASA CR-159053, July 1979 (competition sensitive).

[6] Doherty, C.S. and Butzel, L.M., "STOL Aircraft Structural Vibration Prediction Method," AFFDL-TR-793111, Aug. 1979.

[7] Sussman, M.B., Reed, J.B., O'Keefe, J.V., and Eldridge, W.M., "USB Environmental Assessment Based on YC-14 Flight Test Measurements," Paper presented at AIAA/NASA Ames V/STOL Conference, NASA Ames Research Center, May 23-26, 1977.

[8] Butzel, L.M., Jacobs, L.D., O'Keefe, J.V., and Sussman, M.B., "Cabin Noise Behavior of a USB STOL Transport," AIAA Paper 77-1365, Oct. 1977.

[9] Brown, W.H. and Gison, J.S., "Noise Characteristics of Upper Surface Blown Configurations; Experimental Programs and Results," NASA CR-145143, Oct. 1977.

[10] Rudder, F.F. and Plumblee, H.E., "Sonic Fatigue Design Guide for Military Aircraft," AFFDL-TR-112, May 1975.

[11] Dunn, D.G., Butzel, L.M., DeBlasi, A., Filler, L., and Jacobs, L.D., "Aircraft Configuration Noise Reduction," Vol. I, "Engineering Analysis," Rept. FAA-RD-76-76, June 1976.

[12] Tibbetts, J.G., "Near Field Noise Prediction for Aircraft in Cruising Flight—Methods Manual," NASA CR-159105, Aug. 1979.

[13] Swift, G. and Mungur, P., "A Study of the Prediction of Cruise Noise and Laminar Flow Control Noise Criteria for Subsonic Air Transports," NASA CR-159104, Aug. 1979.

[14] Tibbetts, J.G., "A Computer Program for the Prediction of Near Field Noise of Aircraft in Cruising Flight—User's Guide," NASA CR-159274, June 1980.